Chemical Physics Letters vol. 194, p.252-261 (1992).

Conjugate Peak Refinement : an algorithm for finding reaction paths and accurate transition states in systems with many degrees of freedom.

Stefan Fischer and Martin Karplus.

Committee on Higher Degrees in Biophysics and Department of Chemistry
Harvard University
12 Oxford St., Cambridge, Massachusetts 02138, USA.

Abstract

An algorithm is presented for determining multi dimensional reaction coordinates between two known conformers. Only the energy function and its gradient are required. The resulting paths follow the adiabatic energy valleys and have energy maxima that are true saddle-points, which can be multiple along each path. The method is suitable for the study of complex isomerization reactions, including allosteric transitions in proteins and more general conformational changes of macromolecules.

1. Introduction

Empirical energy functions are being used increasingly to study macromolecules and other systems with a very large number of degrees of freedom [1, 2]. The first step in exploring the topology of the high dimensional energy surface of such systems is to search for the local minima that correspond to stable molecular conformations [3]. It is then necessary to locate the saddle-points that separate these minima and to find the adiabatic reaction path connecting them (also known as the minimum energy path), which is defined as the set of points connecting a saddle-point to a minimum while following the gradient. While there are many efficient algorithms to find local minima, even on a surface of high dimensionality [4], the determination of reaction coordinates and transition states is still a difficult procedure when the objective is to find a path that connects two specific conformers.

Existing methods for determining such paths fall into two categories. Focal methods modify a single conformer until it becomes the saddle-point, of which it is assumed that there is only one along the path between the two minima [5, 6, 7, 8, 9]. Such methods either make use of the second derivative matrix [5, 6], which limits them to low-dimensional problems, or rely on the assumption that the path near the saddle-point has some predetermined shape [7, 8, 9], which limits them to simple energy surface topologies. By design, these methods cannot find paths with multiple transition states. Global methods treat the entire path as a succession of points in conformation space [10, 11]. These points are simultaneously minimized, under constraints that keeps them from falling into nearby minima, until they reach the adiabatic valley connecting the reactant to the product conformers. Such methods do not provide an accurate value for the saddle-point, since the surrounding path-points tend to lie as low as possible on each side of the saddle-point. Therefore, these methods must be supplemented with one of the focal methods to determine each saddle-point.

While finding the adiabatic path itself is desirable, it can easily be obtained by a steepest descent procedure once the saddle-points have been determined [8, 12]. Because of the exponential dependence of the reaction rate on the energy barrier along a given path, knowing the precise height of the saddle-point is important for distinguishing between several conceivable paths. Hence, the saddle-point is the key to the full

characterization of a reaction coordinate. The Conjugate Peak Refinement (CPR) algorithm introduced here is explicitly optimized for finding a series of true saddle-points, which are connected to one another through the adiabatic paths that descend from them and form a continuous reaction coordinate between a specified reactant and product. It is the only available method that will do so reliably for systems with a very large number of degrees of freedom and on highly complex energy surfaces. The method requires a continuous energy function and its first derivative (e.g., of the type used in molecular mechanics simulations), but does not need the second derivatives. The minimum input consists of the reactant and product structures, between which a reaction path is to be determined. The method can also refine an initial guess for the reaction path, such as selected steps along a molecular dynamics trajectory or some other intermediate conformations. The resulting output is a string of points in conformation space that follows the neighborhood of the adiabatic valleys. Any point that is a local maximum along the path will have completely converged to a saddle-point of the energy surface. If the reaction path involves multiple transition states, each of them will have its saddle-point included along the refined path. The final number of path points does not need to be specified before starting the refinement, as the procedure adds them as dictated by the complexity of the energy surface and by the path curvature. Therefore, the density of points along the refined path is not constant and is higher where the path crosses saddle regions or where the adiabatic path has a small radius of curvature.

These properties of simultaneous convergence to multiple saddle-points, automatic adaptation of path-resolution to the energy surface topology and robustness in high-dimensional systems make the CPR method a useful addition to existing approaches. The CPR algorithm has been applied to isomerization reactions in a wide range of molecules, including proteins (e.g. the lid-transition in triosephosphate isomerase [13]). The method is illustrated by employing it on a two-dimensional potential surface. Then the method is applied to the proline ring-puckering reaction in the cyclic decapeptide antamanide.

2. Method

The CPR method relies upon Sylvester's inertia theorem [14], which states that for any set of basis vectors $\boldsymbol{s}_j$ ($j = 0, \ldots, D-1$), conjugate with respect to a Hessian matrix $\boldsymbol{H}$ (the matrix of the second derivatives of the energy) of dimension D (i.e., $\boldsymbol{s}_i^T \boldsymbol{H} \boldsymbol{s}_j = 0$, $\forall\ i \neq j$), the number r_- of such vectors for which

$$\boldsymbol{s}_i^T \boldsymbol{H} \boldsymbol{s}_i < 0 \quad (i = 0, \ldots, r_- - 1) \tag{1}$$

is independent of the choice of the basis-set. Because $\boldsymbol{H}$ is hermitian, its eigenvectors form a conjugate basis set. By definition, the Hessian matrix at a true saddle-point, $\boldsymbol{H}_s$, has exactly one negative eigenvalue, so that $\boldsymbol{H}_s$ has $r_- = 1$. This means that in the vicinity of a saddle-point, for any set of vectors $\boldsymbol{s}_j$ conjugate with respect to $\boldsymbol{H}_s$, there will be one direction $\boldsymbol{s}_0$ along which the energy has a local maximum,

$$\boldsymbol{s}_0^T \boldsymbol{H}_s \boldsymbol{s}_0 < 0 \tag{2a}$$

and $D-1$ directions along which the energy has a local minimum,

$$\boldsymbol{s}_j^T \boldsymbol{H}_s \boldsymbol{s}_j > 0 \quad j > 0 \ . \tag{2b}$$

To converge to a saddle-point from a distance at which the energy can be approximated by a quadratic expansion around that saddle-point,

$$E(\boldsymbol{x}) \approx E(\boldsymbol{x}_s) + \tfrac{1}{2} (\boldsymbol{x} - \boldsymbol{x}_s)^T \boldsymbol{H}_s (\boldsymbol{x} - \boldsymbol{x}_s) \ ,$$

it is necessary to obtain a set of conjugate vectors, of which $\boldsymbol{s}_0$ obeys Eq. (2a), so as to be able to maximize the energy along $\boldsymbol{s}_0$ and to minimize the energy along the remaining directions $\boldsymbol{s}_j$ ($j > 0$). Once a direction along which the energy has a local maximum is found, this direction can be taken as $\boldsymbol{s}_0$. The rest of the conjugate basis-set is then built recursively, making use of a formula by Beale [7, 15], which constructs a set of conjugate directions, starting with an arbitrary direction $\boldsymbol{s}_0$:

$\boldsymbol{s}_0$ (given)

$$\boldsymbol{s}_1 = -\boldsymbol{g}_1 + \frac{\boldsymbol{g}_1^T \boldsymbol{h}}{\boldsymbol{s}_0^T \boldsymbol{h}} \boldsymbol{s}_0$$

$$\boldsymbol{s}_j = -\boldsymbol{g}_j + \frac{\boldsymbol{g}_j^T \boldsymbol{h}}{\boldsymbol{s}_0^T \boldsymbol{h}} \boldsymbol{s}_0 + \frac{|\boldsymbol{g}_j|^2}{|\boldsymbol{g}_{j-1}|^2} \boldsymbol{s}_{j-1} \qquad j > 1 \ ,$$

where $\boldsymbol{g}_j$ is the gradient vector at the energy extremum $\boldsymbol{y}_j$ along $\boldsymbol{s}_{j-1}$ and $\boldsymbol{h}$ is an estimate of $\boldsymbol{H}\boldsymbol{s}_0$. One cycle of maximizing the energy along $\boldsymbol{s}_0$ and minimizing along the successive $\boldsymbol{s}_j$ ($j > 0$) yields the saddle-point on a quadratic energy surface. Sinclair and Fletcher [7] have successfully used this approach to locate single saddle-points on non-quadratic surfaces, by taking $\boldsymbol{s}_0$ as the vector going from the reactant to the product, $\boldsymbol{s}_0 = (\boldsymbol{x}_\mathrm{P} - \boldsymbol{x}_\mathrm{R})$, and iterating through several such maximization/minimization cycles. The fixed choice of $\boldsymbol{s}_0$ in that focal method limits the application of their algorithm to simple energy surfaces, for which $\boldsymbol{H}_\mathrm{s}$ obeys

$$(\boldsymbol{x}_\mathrm{P}-\boldsymbol{x}_\mathrm{R})^T \boldsymbol{H}_\mathrm{s} (\boldsymbol{x}_\mathrm{P}-\boldsymbol{x}_\mathrm{R}) < 0 \ .$$

While the CPR method also makes use of Beale's formula to build conjugate directions, it avoids the limitation on $\boldsymbol{H}_\mathrm{s}$ by adding intermediate path points on each side of the saddle, so as to introduce progressively better choices of $\boldsymbol{s}_0$. At a given stage of refinement, the reaction path is described by a set of n points $[\boldsymbol{x}_1, \boldsymbol{x}_2, \ldots, \boldsymbol{x}_n]$, each corresponding to a molecular conformation with its coordinates represented by a vector of dimension $D = 3N$ (N = number of atoms); here $\boldsymbol{x}_1$ is the reactant conformation, $\boldsymbol{x}_n$ is the product and $\boldsymbol{x}_i$ ($i = 2, \ldots, n-1$) are any intermediate conformers along the path. The path segments between the points are constructed by interpolating linearly between point $\boldsymbol{x}_i$ and $\boldsymbol{x}_{i+1}$ ($i = 1, \ldots, n-1$). The choice of polarity of the reaction (i.e. whether $\boldsymbol{x}_1$ or $\boldsymbol{x}_n$ is defined as the reactant) is arbitrary and does not affect the results. CPR is an iterative procedure, in which a single intermediate point is either added, refined or removed during a given cycle, until the only local maxima in energy left along the path are true saddle-points.

We now demonstrate how the CPR procedure works by following the progress of a path refinement on the two-dimensional potential described by Müller and Brown [8] (Fig. 1); the algorithmic details will be presented elsewhere. The initial guess consists of the points corresponding to the reactant $\boldsymbol{r}$ and the product $\boldsymbol{p}$ (Fig. 1A). A coarse set of

steps along the line segment from $\boldsymbol{r}$ to $\boldsymbol{p}$ reveals the presence of an energy maximum around point $\boldsymbol{y}_0^1$, so that $\boldsymbol{s}_0$ is chosen in the first cycle as $\boldsymbol{s}_0 = (\boldsymbol{p} - \boldsymbol{r})$. Thorough maximization in term of α along the line $\boldsymbol{r} + \alpha\boldsymbol{s}_0$ yields $\boldsymbol{y}_1^1$. A line-minimization is carried out from $\boldsymbol{y}_1^1$ along the conjugate vector $\boldsymbol{s}_1$, to obtain $\boldsymbol{x}_1$. If the refinement were continued as a Sinclair-Fletcher saddle-point search, the next cycle would start with a maximization along the line $\boldsymbol{x}_1 + \alpha\boldsymbol{s}_0$, keeping $\boldsymbol{s}_0$ unchanged. Because there is no local maximum along that line (the only maxima are at infinity), the Sinclair-Fletcher algorithm would fail on the Müller-Brown potential. In the CPR method, $\boldsymbol{x}_1$ becomes a new intermediate along the path, which now has two segments (Fig. 1B). Starting the second cycle of refinement, the search for the point of highest energy is performed along the whole path $[\boldsymbol{r}, \boldsymbol{x}_1, \boldsymbol{p}]$. No local maximum is found between $\boldsymbol{r}$ and $\boldsymbol{x}_1$, but there is a peak at $\boldsymbol{y}_1^2$, between $\boldsymbol{x}_1$ and $\boldsymbol{p}$, so that $\boldsymbol{s}_0$ is now taken as $\boldsymbol{s}_0 = (\boldsymbol{p} - \boldsymbol{x}_1)$. A conjugate line-minimization from $\boldsymbol{y}_1^2$ gives an additional path intermediate $\boldsymbol{x}_2$, which satisfies the following two conditions. First, the RMS-gradient of the energy at $\boldsymbol{x}_2$ is essentially zero. Second, even though $\boldsymbol{x}_2$ is the result of *D-1* line-minimizations (here $D = 2$), it is still a local energy maximum along the path, so that by construction it satisfies Eqs. (2a) and (2b). Consequently, point $\boldsymbol{x}_2$ qualifies as a saddle-point. If these conditions were not satisfied and $\boldsymbol{x}_2$ was still the peak of the path, then another cycle of refinement of $\boldsymbol{x}_2$ would be required; this does happen in cycle 4 (see below). In the third cycle (Fig. 1C), another energy peak is found between $\boldsymbol{x}_2$ and $\boldsymbol{p}$. Maximization along $\boldsymbol{s}_0 = (\boldsymbol{p} - \boldsymbol{x}_2)$ to $\boldsymbol{y}_1^3$, followed by line-minimization along $\boldsymbol{s}_1$, yields the third intermediate path-point $\boldsymbol{x}_3$. The RMS-gradient at $\boldsymbol{x}_3$ is small, indicating that it is close to a stationary point. In the fourth refinement cycle (Fig. 1D), the peak in energy along the four segments of the path is found to be $\boldsymbol{x}_3$ itself. To refine such a point, $\boldsymbol{s}_0$ is taken as the direction $\boldsymbol{t}_3$ which bisects the two segments that meet at $\boldsymbol{x}_3$,

$$\boldsymbol{t}_3 \equiv \frac{\boldsymbol{x}_+ - \boldsymbol{x}_3}{|\boldsymbol{x}_+ - \boldsymbol{x}_3|} - \frac{\boldsymbol{x}_- - \boldsymbol{x}_3}{|\boldsymbol{x}_- - \boldsymbol{x}_3|} \quad ,$$

where $\boldsymbol{x}_-$ and $\boldsymbol{x}_+$ are the path-points on each side of $\boldsymbol{x}_3$, here $\boldsymbol{x}_2$ and $\boldsymbol{p}$, respectively. This vector $\boldsymbol{t}_i$ can be interpreted as the direction "tangent" to the path at $\boldsymbol{x}_i$. After maximizing locally in the neighborhood $\boldsymbol{x}_3$ along $\boldsymbol{s}_0 = \boldsymbol{t}_3$, a conjugate minimization yields $\boldsymbol{x}_3'$, which replaces $\boldsymbol{x}_3$ as the intermediate path-point between $\boldsymbol{x}_2$ and $\boldsymbol{p}$ and also qualifies as a saddle-point. At this stage, the only local maxima along the path $[\boldsymbol{r}, \boldsymbol{x}_1, \boldsymbol{x}_2, \boldsymbol{x}_3', \boldsymbol{p}]$ are saddle-points, so that the refinement is complete.

Steepest descent minimization on each side of the saddle-point $\boldsymbol{x}_2$ connects $\boldsymbol{r}$ to the stable intermediate $\boldsymbol{i}$. Steepest descent on each side of the other saddle-point $\boldsymbol{x}_3'$ connects $\boldsymbol{i}$ to $\boldsymbol{p}$. This gives the full adiabatic path from $\boldsymbol{r}$ to $\boldsymbol{p}$.

Because the dimensionality in this example is $D = 2$, $\boldsymbol{s}_{D-1}$ is the one and only direction conjugate to $\boldsymbol{s}_0$, so that the number of successive line-minimizations in a given cycle is always $D-1$. In molecular systems with several hundred degrees of freedom, the number of successive line-minimizations cannot always be allowed to reach $D-1$. Due to the non-quadratic nature of molecular potential functions, minimization along all $D-1$ recursively built $\boldsymbol{s}_j$ could result in the point $\boldsymbol{y}_j$ falling into a nearby minimum. To prevent this, line-minimizations are interrupted as soon as the projection τ_j onto $\boldsymbol{s}_0$ of the gradient $\boldsymbol{g}_j$ at $\boldsymbol{y}_j$ exceeds a certain tolerance μ, defined by

$$\tau_j \equiv D^{1/2} \frac{\boldsymbol{g}_j^T \boldsymbol{s}_0}{|\boldsymbol{g}_j| \cdot |\boldsymbol{s}_0|} > \mu \qquad (j > 1).$$

Sinclair and Fletcher [7] use the same criterion in their saddle-search, except that they do not correct for dimensionality. This becomes necessary when dealing with very large systems. Point $\boldsymbol{y}_j$ then becomes a new path intermediate in the usual way. Even though not all $D-1$ line-minimizations are performed, the resulting point $\boldsymbol{y}_j$ is closer to the adiabatic valley than the path-point $\boldsymbol{y}_1$ it replaces, leading to an improved path.

In cycles where the energy peak along the path is one of the path intermediates $\boldsymbol{x}_i$ (as in cycle 4 of Fig. 1), it can sometimes happen that no local energy maximum around $\boldsymbol{x}_i$ can be found along the "tangent" $\boldsymbol{t}_i$. Since a direction $\boldsymbol{s}_0$ is not determined in such a case, the point $\boldsymbol{x}_i$ is removed from the series of intermediates and the path is rebuilt between the two points that surrounded $\boldsymbol{x}_i$. This behavior is more likely to happen in a system with $D \gg 2$, where path intermediates resulting from less than $D-1$ conjugate line-minimizations in early refinement cycles can be neighbors to more recent points which are closer to the bottom of the adiabatic valley.

3. Applications

The CPR algorithm has been integrated into the program CHARMM [16], which provides the empirical energy function, and applied to conformational transitions in a range of molecules, involving up to several thousand degrees of freedom (to be published). Here, we consider the transition between the two pucker states of the five membered ring of a proline residue. We first examine the transition in an unhindered pyrrolidine ring and then compare this result with the behavior of one of the prolines in the cyclic decapeptide antamanide, whose dynamics have been studied recently [17].

3.1 N-acetyl-pyrrolidine (NAP)

NAP is an analogue of a peptidyl-proline fragment. Its structure is given in Figure 2. Using a polar hydrogen model (PARAM19), in which non-polar hydrogens are combined with their bonded carbons into a single extended center [16], NAP has 8 atoms and 24 degrees of freedom in the full Cartesian coordinate space. In this model, the minimum energy conformers of NAP have their heavy atoms lying in one plane, except for carbons β and γ. This ring pucker allows for two conformers, related through a plane of symmetry, which differ only in whether carbon β is above the plane and carbon γ is below or vice-versa. These two conformers correspond to the reactant and the product of the reaction considered here. Although there are a variety of ways of describing the ring pucker (e.g. pseudorotation coordinates [18]), we use two of its dihedral angles, χ_1 and χ_3 (Fig. 2), because these readily accessible internal coordinates provide a good separation

of the ring's stationary points and highlight its symmetry. The values of $[\chi_1, \chi_3]$ corresponding to the two minima are [*-37.6*, *-37.5*] and [*37.6*, *37.5*]. As can be seen in Figure 3 and is expected from Figure 2, the potential energy surface is nearly centro-symmetric.

Figure 3 details the refinement of the reaction path. While the adiabatic energy map in terms of internal coordinates χ_1 and χ_3 looks deceptively simple, the actual refinement progresses on an energy surface defined in Cartesian coordinate space, which spans 24 dimensions. The adiabatic path is also more curved in that space. For this reason the path refinement is not dictated by the features of the adiabatic $[\chi_1, \chi_3]$ map as it was on the Müller-Brown potential, which was the actual surface on which the CPR progressed. To clarify how the algorithm perceives the topology of the surface in Cartesian coordinates, we plot the energy profile along the path segments for each refinement cycle (Figure 4).

Starting from a linear interpolation between reactant ***r*** and product ***p***, an intermediate point ***a*** is added after 23 conjugate line-minimizations in the first cycle (*D-1* = 23 is the maximum number of line-minimizations per cycle) and further refined to ***a***' with 23 more line-minimizations in cycle 2 (Fig. 3A). Intermediates ***b*** and ***c*** are added on each side of ***a***' in cycles 3 and 4, which take only 3 line-minimizations, because $\tau_4 > \mu$ in both cycles (Fig. 3B). In cycle 5, a local energy maximum cannot be found on the tangent to the path at ***a***', which at this stage is the peak along the path. Point ***a***' is therefore removed, resulting in a single path segment connecting point ***c*** to ***b*** (Fig. 3C). Finally, point ***d*** is added after 23 line-minimizations in cycle 6, with a RMS-gradient of only *0.4* kcal/molÅ, indicating that ***d*** is quite close to the saddle-point (Fig. 3C). More cycles refine point ***d*** further (not shown), reducing its RMS-gradient by an order of magnitude at every iteration. After 5 more cycles of 23 line-minimizations, the RMS-gradient is less than $8 \cdot 10^{-7}$ kcal/molÅ. This vanishing gradient and a normal-mode analysis at point ***d*** revealing only one imaginary frequency ($\nu = 164$ cm^{-1}) confirms that ***d*** is a saddle-point. The activation barrier along the refined path is *3.26* kcal/mol, as compared with *11.9* kcal/mol along the initial line-interpolation between ***r*** and ***p***. The

whole refinement took less than 2 CPU seconds (all CPU times herein are given for one processor on a Convex 220).

In the transition state, $[\chi_1, \chi_3]_s = [-21.7, 22.0]$. Because of the asymmetry of the CH_3CO group, χ_1 does not exactly equal $-\chi_3$. The ring structure is that of an open envelope, with all 4 carbon atoms in one plane and the nitrogen out of that plane (the C_α—N—C_δ plane being the "flap" of the envelope). As can be seen from the adiabatic map in Figure 3, there are two such transition states in the pyrrolidine ring, which are related by a plane of symmetry and have with their "flap" on either side of that plane. Each connects ***r*** to ***p*** via a different, although symmetrical reaction path. When the ring is placed in an anisotropic environment, or the torsion about the dihedral angle ϕ is restricted by an outgoing polypeptide chain, this symmetry is broken. An example of this is shown in the following section.

3.2 Proline 2 in antamanide

The antamanide molecule, whose X-ray structure [19] has been determined and solution structure has been analyzed by NMR [17], is a cyclic decapeptide of sequence $-Val_1$-Pro_2-Pro_3-Ala_4-Phe_5-Phe_6-Pro_7-Pro_8-Phe_9-Phe_{10}- , which consists of 90 atoms in the polar hydrogen model. All 270 degrees of freedom were allowed to contribute to the reaction coordinate. We chose to explore the puckering behavior of proline 2. The energy minima correspond to $[\chi_1, \chi_3]$ values in proline 2 of $[-34.4, -38]$ for the reactant and $[25.8, 42.8]$ for the product state, the latter being *1* kcal/mol higher with the CHARMM potential energy. This difference in geometry and energy between the two puckering states is evidence that the symmetry of the energy surface describing the ring is broken in proline 2, as compared with NAP (section 3.1).

To determine the extent of this loss in symmetry, we performed two path refinements to find the transition states of the puckering reaction. Each refinement was started with an intermediate close to one of the two saddle-points in NAP. The antamanide intermediate of refinement A was prepared by constraining the $[\chi_1, \chi_3]$ dihedral angles of proline 2 at $[-22, 22]$ and letting the rest of the molecule relax. For the intermediate of refinement B, these dihedral angles were preset to $[22, -22]$. The two resulting paths (shown in Fig. 5) cross the same saddle-point, which is located at

$[\chi_1, \chi_3]_S = [-17.7, 11.2]$. The activation barrier is *3.84* kcal/mol relative to the reactant and there is a unique imaginary saddle-frequency of *208.8* cm^{-1}. Partial path refinement required only *37* (for A) and *122* (for B) line-minimizations (taking *5.5* and *19.5* CPU seconds), achieving an energy barrier within *0.06* kcal/mol of its final value and a RMS-gradient at the saddle-point of less than $5 \cdot 10^{-2}$ kcal/molÅ. After a total of *8* and *28* cycles, involving a total of *602* and *729* conjugate line-minimizations (taking *62* and *78* CPU seconds) for A and B respectively, the RMS-gradient at the saddle was finally less than $1.6 \cdot 10^{-6}$ kcal/molÅ.

Because the CPR method gives the exact saddle-points, it was possible to conclude that the two refined paths are identical by simply comparing the energies at the saddle-points (the difference in final energy between saddle A and saddle B is less than 10^{-9} kcal/mol). The fact that only one possible reaction path exists, indicates that the force-field of the proline 2 ring in the $[\chi_1, \chi_3] = [22, -22]$ region is significantly perturbed from that present in NAP. This was verified by calculating the adiabatic energy map, which is overlaid on the reaction paths in Figure 5. The effect of the polypeptide environment is to destabilize one of the intrinsic saddle-points of the isolated ring, so as to make it disappear. Again, the adiabatic path can be obtained at any desired resolution by steepest descent minimization on each side of the saddle-point.

4. Discussion

The Conjugate Peak Refinement (CPR) is a global method, in the sense that it handles the whole path explicitly. However, it does not treat all the points along the path equally at all times, relaxing them simultaneously into the adiabatic valley, as do other global methods [10, 11]. Instead, the approach of the CPR algorithm is to recognize and eliminate non-optimal parts of a reaction path. This is done by searching for energy "hot-spots" along the path and bringing these path regions down into a nearby valley linking the saddle-points. By alternating controlled conjugate minimization with path rebuilding, the method simultaneously achieves relaxation of the path into the valleys and convergence of the path maxima to the connecting saddle-points of the energy surface.

Obtaining the saddle-points is an essential step in characterizing and evaluating a reaction path. It directly provides the energy barrier and the adiabatic path (by steepest descent). Moreover, it makes it possible to perform a normal-mode analysis, in which the eigenvector associated with the unique negative eigenvalue represents the reactive mode at the transition state. Examination of this mode helps to determine the extent of coupling among the parts of the reactive system and to isolate the degrees of freedom that contribute the most to a complex reaction coordinate. The resulting reaction coordinate can then be used in free energy simulations to calculate the activation barrier [20] and in activated dynamics simulations to compute the transmission coefficient [21]. Having isolated the true saddle-point also guarantees that the path is fully refined and is not crossing a degenerate (multiple negative eigenvalues) saddle region, as has been observed in one global method [10a].

Other positive aspects are that the CPR method does not impose any a priori restrictions on path length and shape, that computational resources are concentrated on improving the reactive path in its more relevant high-energy segments and that the transition state highest in energy (i.e. rate limiting) is isolated first, before the refinement proceeds with improving path segments in regions of lower energy. This last feature can be particularly useful when searching for a globally optimal path by performing multiple path refinements with different initial guesses. In such a case, each refinement would only be carried out until the rate-limiting saddle-point is found, without further refining the lower segments of the trial path.

The method could be optimized to take advantage of the form of a particular energy function by the proper choice of coordinate representation. Since energy and gradient evaluations are frequent during the phase of conjugate minimization, a coordinate system in which the potential function and its derivative are easily obtained would be most suitable. For example, Cartesian coordinates are a good choice if the potential has pair-wise interaction terms. On the other hand, the interpolations along path-segments are best done in a coordinate system that naturally follows the adiabatic valleys of the potential, since this will greatly reduce the number of intermediate path-points to be refined. Internal coordinates, for instance, would be appropriate if the potential has valence terms. An example of this can be seen in cycle 2 of Fig. 4, where interpolation in Cartesian space leads to spurious energy barriers on each side of point ***a'***, largely due to covalent deformation. These barriers must then be removed by adding two extra intermediates, ***b*** and ***c***, in subsequent cycles. Because force-fields for macromolecules contain both pair-wise (non-bonded) and valence (bonded) terms, an implementation of the algorithm in a hybrid coordinate representation is planned, with Cartesian coordinates used during conjugate minimizations and internal coordinates used to define the interpolating path-segments that are searched for peaks in the energy.

Acknowledgments

We would like to thank R. Brüschweiler, B. Roux, J. Straub and N. Summers for valuable discussions. This work was supported in part by a grant from the National Science Foundation. The calculations were done on a VAX 11-780 and a CONVEX 220.

References

(1) **C. L. Brooks, M. Karplus, B. M. Pettitt**. Proteins: a theoretical perspective of dynamics, structure and thermodynamics. In: Advances In Chemical Physics, vol. 71 (John Wiley & Sons, New York, 1988).

(2) **J. A. McCammon, S. Harvey.** Dynamics of proteins and nucleic acids. (Cambridge University Press, Cambridge, 1987).

(3) **R. Elber, M. Karplus.** Science 235 (1987) 318.

(4) **W. H. Press, B. P. Flannery, S. A. Teukolsky, W. T. Vetterling.** Numerical Recipes: the art of scientific computing (Cambridge Univ. Press, Cambridge, 1986).

(5) **C. J. Cerjan, W. H. Miller.** J. Chem. Phys. 75 (1981) 2800.

(6) **S. Bell, J. S. Crighton, R. Fletcher.** Chem. Phys. Letters 82 (1981) 122.

(7) **J. E. Sinclair, R. Fletcher.**J. Phys. C: Solid St. Phys. 7 (1974) 864.

(8) **K. Müller, L. D. Brown.** Theoret. Chim. Acta 53 (1979) 75.

(9) **S. Bell, J. Crighton.** J. Chem. Phys. 80 (1984) 2464.

(10) **R. Elber, M. Karplus.**Chem. Phys. Letters 139 (1987) 375.
A. Ulitsky, R. Elber. J. Chem. Phys. 92 (1990) 1510.
R. Czerminski, R. Elber. Int. J. Quantum Chem. 24 (1990) 167.

(11) **L. R. Pratt.** J. Chem. Phys. 85 (1986) 5045.

(12) **R. S. Berry, H. L. Davis, T. L. Beck.** Chem. Phys. Letters 147 (1988) 13.

(13) **D. Joseph, S. Fischer, M. Karplus.** Work in progress.

(14) **I. N. Herstein.** Topics in algebra, 2nd ed. (John Wiley & Sons, New York, 1975).

(15) **E. M. L. Beale**. Numerical methods for non-linear optimization (Editor F. A. Lootsma, London: Academic Press, 1972).

(16) **Bernard R. Brooks & al.** J. of Computational Chemistry 4 (1983) 187.

(17) **R. Brüschweiler, B. Roux, M. Blackledge, C. Griesinger, M. Karplus, R. R. Ernst.** J. Am. Chem. Soc., in press.

(18) **C. Altona, M. Sundaralingam.** J. Am. Chem. Soc. 94 (1972) 8205.

(19) **I. L. Karle & al.** PNAS 76 (1979) 1532.

(20) **S. H. Northrup, M. R. Pear, C.-Y. Lee, J. A. McCammon, M. Karplus.** PNAS 79 (1982) 4035.
R. Elber. J. Chem. Phys. 93 (1990) 4312.

(21) **B. J. Berne**, **M. Borkovec, J. E. Straub**. J. Phys. Chem. 92 (1988) 3711.

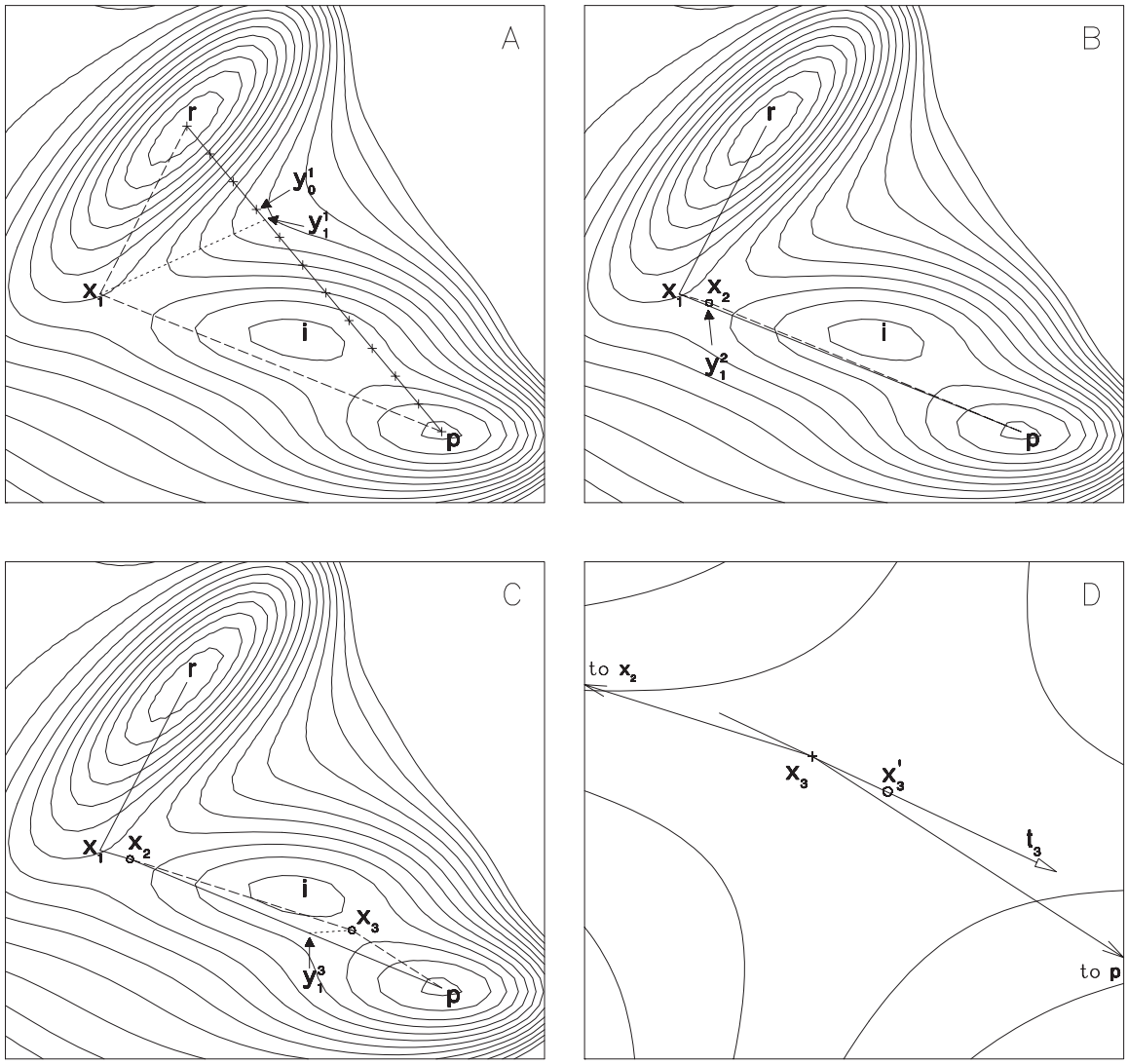

Figure 1. Path refinement progress on a Müller-Brown potential [8]. Panels A through D correspond to cycle 1 through 4 of the CPR iterations (see Method's section). The reactant, product and intermediate wells are indicated with **r**, **p** and **i**. Panel D is an enlargement of the saddle-region between **i** and **p**. The current path segments at the beginning of a given cycle are in solid lines. The newly build segments are in dashed lines. The conjugate directions $\boldsymbol{s}_1$ are in dotted line. Saddle-points are marked with a circle.

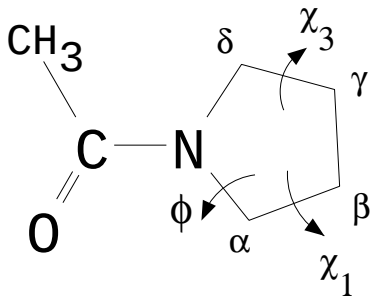

Figure 2. N-acetyl-pyrrolidine.

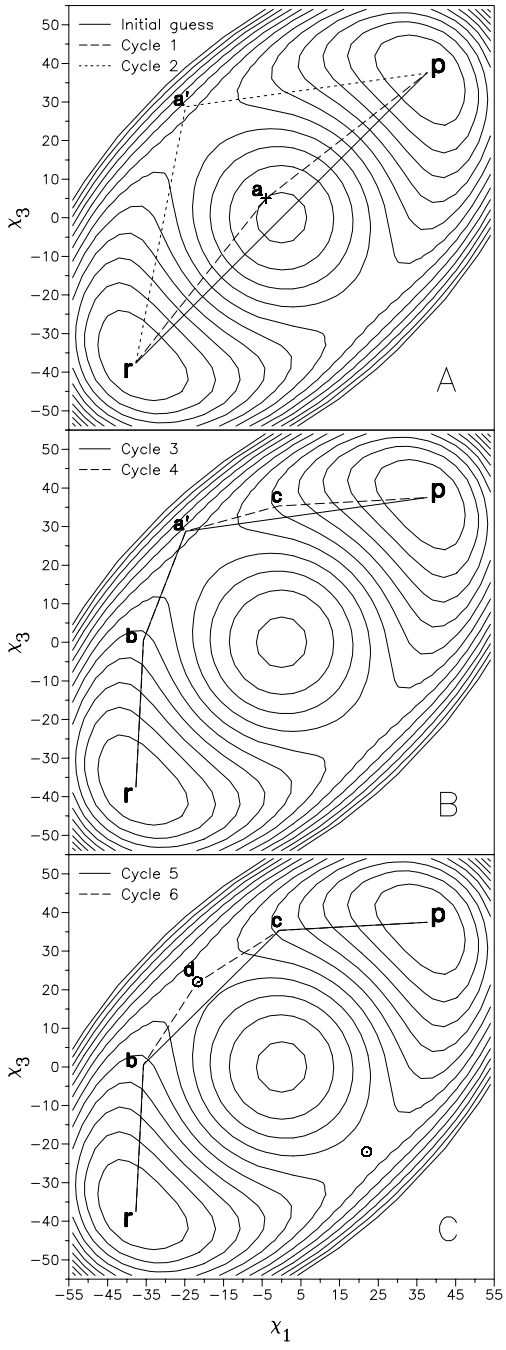

Figure 3. The path at successive stages of refinement, for the ring-puckering reaction in NAP. Adiabatic energy map (contour lines plotted every 0.5 kcal/mol) as a function of the dihedral angles χ_1 and χ_3 (in degrees). The saddle-points are indicated by a circle. A: Initial guess (—), cycle 1 (----), cycle 2 (·····). B: Cycle 3 (—), cycle 4 (----). C: Cycle 5 (—), cycle 6 (----).

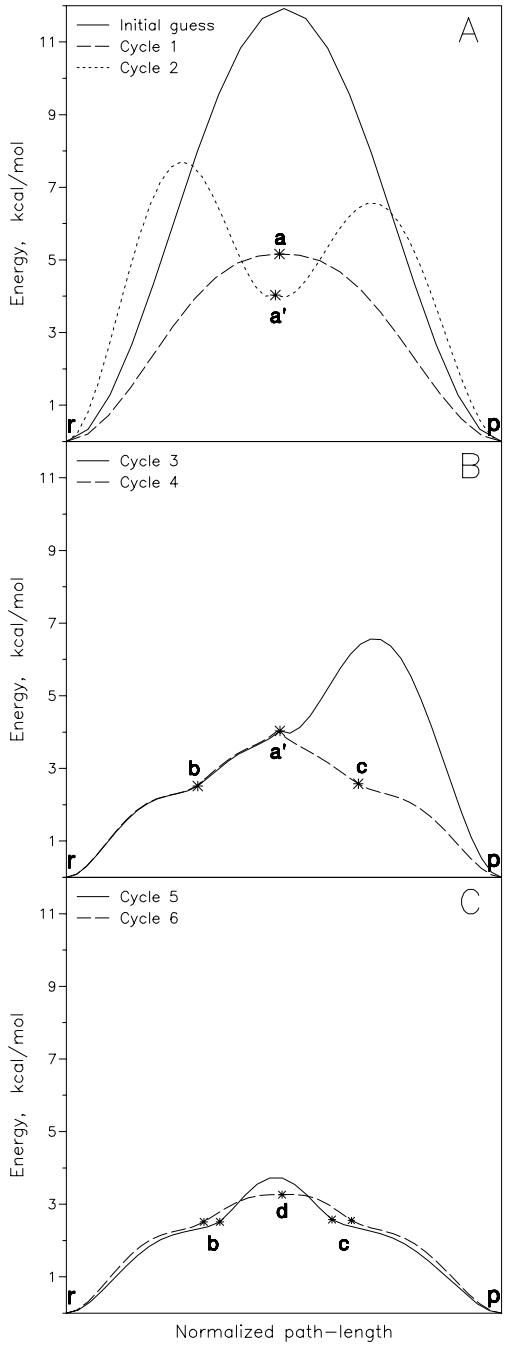

Figure 4. The energy along the NAP ring-puckering path. Panel and cycle numbering is the same as in Fig. 3. The energy is evaluated along the line-segments that interpolate in Cartesian coordinate space between the path-points (which are marked with an asterisk). The horizontal axis is the distance along that curvilinear path, normalized by the total length L of the path, $L = \sum_{i=2}^{n} |\boldsymbol{x}_i - \boldsymbol{x}_{i-1}|$. A: Initial guess (——), cycle 1 (----), cycle 2 (·····). B: Cycle 3 (——), cycle 4 (----). C: Cycle 5 (——), cycle 6 (----).

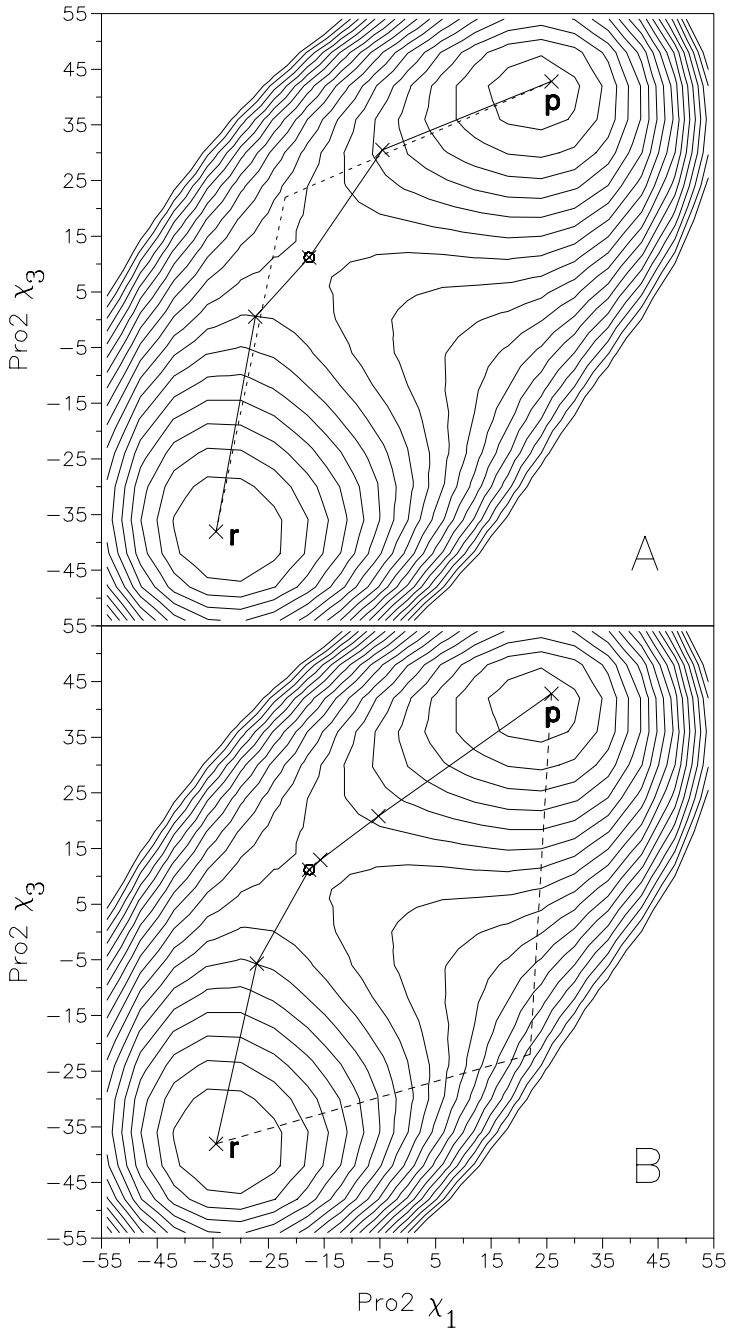

Figure 5. Panels A and B show the input (dotted lines) and refined (solid lines) paths of two independent path refinements in antamanid, as a function of the dihedral angles χ_1 and χ_3 in proline 2. Path-points are marked with an □ and the saddle-point is indicated by a circle. The contour lines in the adiabatic energy map are plotted every 0.5 kcal/mol.